designs

MDPI

Article

Influence of Topological Defects on the Mechanical Response of Unit Cells of the Tetrachiral Mechanical Metamaterial

Linar Akhmetshin *, Kristina Iokhim, Ekaterina Kazantseva and Igor Smolin

Faculty of Physics and Engineering, National Research Tomsk State University, 634050 Tomsk, Russia; iokhim.k@mail.ru (K.I.); kazantseva.ea@ispms.ru (E.K.); smolin@ispms.ru (I.S.)
* Correspondence: akhmetshin.lr@gmail.com

Abstract: The primary benefit of metamaterials is that their physical and mechanical properties can be controlled by changing the structure geometry. Numerical analysis tools used in this work offer a few advantages over full-scale testing, consisting of an automated process, as well as lower material and time costs. The investigation is concerned with the behavior of unit cells of the tetrachiral mechanical metamaterial under uniaxial compression. The base material is studied within an elastic mathematical model. The influence of topological defects of the unit cell on the metamaterial properties is studied for the first time. Defects, and especially topological defects, play a decisive role in the mechanical behavior of materials and structures. The unit cell without defects reveals orthotropy of properties. Torsion of a cell with a chiral structure is induced by the rotation of all tetrachiral walls, and therefore it is sensitive to the introduction of defects. There are cases of increased torsion as well as of no compression–torsion coupling effect. In the latter case, the unit cell experiences only shear. The effective Young's modulus is calculated to vary in the range from 23 to 57 MPa for unit cells of different topologies. With the successive introduction of defects in two walls, the studied characteristics increase, correlating with each other. A further increase in the number of defects affects the characteristics in different ways. The introduction of two more defects in the walls decreases torsion and increases Young's modulus, after which both characteristics decrease. The introduction of topological defects in all walls of the unit cell leads to the orthotropic behavior of the cell with the opposite sign of torsion.

Keywords: mechanical metamaterial; tension–torsion coupling; compression–torsion properties; deformation mechanism; finite element simulation; architected cellular metamaterials; microstructure–property relationship

Citation: Akhmetshin, L.; Iokhim, K.; Kazantseva, E.; Smolin, I. Influence of Topological Defects on the Mechanical Response of Unit Cells of the Tetrachiral Mechanical Metamaterial. *Designs* **2023**, *7*, 129. https://doi.org/10.3390/designs7060129

Academic Editor: José António Correia

Received: 23 October 2023
Revised: 10 November 2023
Accepted: 10 November 2023
Published: 13 November 2023

1. Introduction

In the last few decades, great interest has been expressed by researchers and representatives of high-tech industries in metamaterials. A separate class of metamaterials is mechanical metamaterials [1–3]. Crystal lattice cells consist of atoms or ions, while metamaterials are composed of much larger cells, orders of magnitude larger than the atom [4]. In fact, mechanical metamaterials are structures composed of certain blocks or elements [3,5]. The metamaterial structure with a great number of such elements can be considered an effective continuous medium [6]. The term "metamaterial" is used for media with effective properties not found in conventional materials [7]. Thus, chiral metamaterials are characterized by torsion under uniaxial loading [8], which is referred to as the tension/compression–torsion coupling effect. This allows the chiral metamaterial to be treated as a micropolar medium [9]. Chirality is a property of asymmetry when an object cannot be mapped to its mirror image by rotations and translations alone. Chirality can be either left-handed or right-handed [10]. A simple chiral element has a central ring and ligaments extending from it [11]. The number of ligaments determines the name of the chiral structure.

For mechanical metamaterials, it is of interest to study their unusual properties and elastic characteristics, such as (1) Young's modulus, (2) shear and bulk moduli of elasticity, and (3) Poisson's ratio [4], symmetric or even asymmetric effective mass density can be physically realized as well [12].

Metamaterial, taken as an effective medium with averaged effective properties, can be described within composite mechanics using the procedure of homogenization of heterogeneous materials with a periodic or random structure [13].

The analogy between classical and metamaterials can be extended to the presence of defects in the studied objects. Plasticity physics extensively studies various types of defects in the crystal structure [14]. On the basis of the analogy between metamaterials and spin systems with ferromagnetic and antiferromagnetic interactions, Meeussen et al. developed an approach to the introduction and analysis of mechanical defects in two- and three-dimensional structures, as well as in arbitrary cells [15]. Consideration for topological defects will enable the control of mechanical properties of metamaterials [16], as well as possible active wave propagation control in metamaterials [12]. The targeted design of microstructure architectures allows the development of materials with optimum mechanical and new functional properties [17,18]. The optimum structural ratios are desirable for use in engineering [1] and biomedicine [19].

The development of orthotropic metamaterials is currently of considerable interest. They are needed in important fields, such as the development of the multimodal resonator combining translational and rotational modes [20]. In addition, metamaterials open up new avenues for broadband sound insulation. The results obtained for two-dimensional chiral metamaterials demonstrate the possibility of designing the micromechanical morphology that provides the desired macroscopic behavior [21]. The orthotropic behavior of metamaterials also affects the bearing capacity of related structures, which should meet the requirements for lightness and high rigidity [22].

Without loss of generality, we can assume that cellular metamaterials have two levels of structural hierarchy. The lower level is represented by a unit cell. As the number of cells increases, the next level of structural hierarchy is considered, i.e., a theoretically continuous medium on the macroscale [23].

Cellular metamaterials consist of a set of unit cells. These cells are connected to each other in a certain way. If the fact that cells are connected by the overlapping method [24] is ignored, a unit cell of the mechanical tetrachiral metamaterial can be taken as the representative volume element.

The present work is devoted to the study of the metamaterial with a tetrachiral structure. The object of investigation is its cubic unit cell, with one ring and four ligaments in each wall. Walls are connected by ligaments at the vertices of the unit cell. The aim of this work is to explore the influence of topological defects on the mechanical response of tetrachiral metamaterials. Attempts are made to find a correlation between the effective mechanical properties of a unit cell of the tetrachiral metamaterial and its microstructural features in order to ensure the programmability of the metamaterial properties. Particular attention is given to the retention of the orthotropy of mechanical properties. The influence of the architectural transformation of one wall of the unit cell on its mechanical response was investigated in the previous work [25]. The novelty of the present paper is in the study of the influence of successive transformations of all walls of the unit cell.

The rest of the paper is organized as follows. Section 2 provides the materials and methods, including information about the tetrachiral structure and unit cell of the metamaterial, properties of the base material from which the metamaterial is built, the mathematical formulation of the problem and boundary conditions, as well as a description of the numerical model for simulation. Section 3 summarizes the results obtained in this computational study on the mechanism of structure rotation and sample torsion and the effective Young's modulus of the metamaterial. Section 4 discusses the correlation between the abovementioned characteristics of the metamaterial, and Section 5 concludes the paper.

2. Metamaterial Structure and Numerical Model

2.1. Tetrachiral Structure and Unit Cell of the Metamaterial

A tetrachiral structure of the unit cell of the metamaterial is shown in Figure 1. It is characterized by five parameters: wall length l and thickness h, ligament width t, outer radius r_2, and inner radius r_1 of the ring. Parameters of the tetrachiral structure used in the study are presented in Table 1.

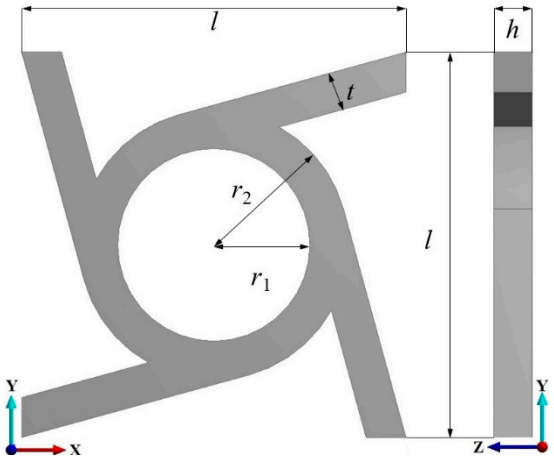

Figure 1. Tetrachiral structure of the metamaterial.

Table 1. Tetrachiral structure parameters used in the study.

l	h	t	r_2	r_1
0 mm	5 mm	5 mm	17.5 mm	12.5 mm

A two-dimensional tetrachiral structure is formed in a solid model with thickness h by extrusion. The unit cell is the smallest repetitive volume of the cellular material, which is composed of specially designed geometric elements that form the structure of the chiral metamaterial. To create a unit cell of the metamaterial, two-dimensional tetrachiral elements should be formed into a three-dimensional figure, a cube in our case. A simple example of the formation of such a cell is shown in Figure 2.

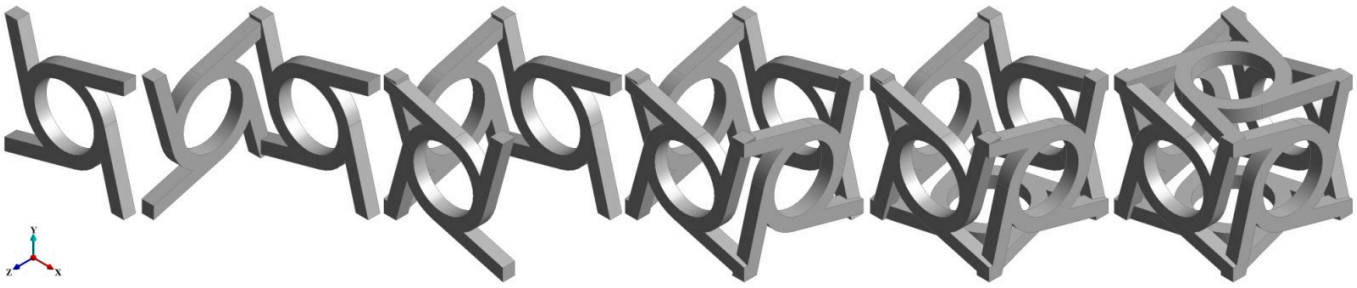

Figure 2. Formation of a metamaterial unit cell.

2.2. Mathematical Model

As mentioned earlier, a metamaterial consisting of unit cells exhibits certain effective properties at the macro level. These effective characteristics can be determined by simulating the mechanical response of a unit cell, which is assumed to consist of structural elements of the metamaterial. These structural elements include a set of connected rectilinear and curvilinear beams, which are made of the base material, namely, a conventional isotropic material or a solid continuous medium. Therefore, the continuum mechanics approach can be used for this purpose.

To simulate the deformation of the unit cell of the tetrachiral metamaterial, the boundary value problem is considered for the system of elastic equations for the fields of displacements u_i and stresses σ_{ij} in a three-dimensional formulation. The system includes equilibrium equations (1), Cauchy relations (2) for determining strains by displacements, and constitutive relations (Hooke's law) (3) relating stresses to strains:

$$\sigma_{ij,j} = 0, \tag{1}$$

$$\varepsilon_{ij} = \frac{1}{2}\left(u_{i,j} + u_{j,i}\right), \tag{2}$$

$$\sigma_{ij} = \lambda \cdot \delta_{ij} \varepsilon_{kk} + 2 \cdot \mu \cdot \varepsilon_{ij}. \tag{3}$$

Here, σ_{ij} is the stress tensor component, ε_{ij} is the strain tensor component, u_i is the displacement vector component, λ and μ are the Lamé constants, δ_{ij} is the Kronecker delta, and the subscripts with a comma denote the partial derivative with respect to the coordinate $i, j = 1, 2, 3$.

The Lamé constants are related to the elasticity modulus E and Poisson's ratio ν by

$$\lambda = \frac{\nu E}{(1+\nu)(1-2\nu)}, \ \mu = \frac{E}{2(1+\nu)}.$$

The base material is assumed to be isotropic and homogeneous, and it is therefore characterized by two material constants. The elastic constants are assumed to have the following values: Young's modulus E = 2.6 GPa and Poisson's ratio ν = 0.4. These values correspond to acrylonitrile butadiene styrene (ABS) plastic. Note that the effective properties of metamaterials depend, to a large extent, not on the elastic modulus values of the base material, but on the macrostructural geometry of the metamaterial.

2.3. Boundary Conditions

Here, consideration is given to the uniaxial compression of the unit cell. One of the walls has rigid boundary conditions, at which zero displacements are set. Mixed boundary conditions are imposed on the opposite wall, allowing for the cell compression perpendicular to this wall and for displacement in the wall plane (the corresponding stress vector components are zero). Thus, this wall can not only move and change its size but also rotate due to ligament deformation and ring rotation. The rest walls have free stress boundary conditions.

For a unit cell compressed by 3% along the Y-axis (Figure 3), these boundary conditions can be written as the following formulae:

$$u_i = 0 \text{ at } x_i \in S_1; \ u_2 = -0.03l \text{ and } \sigma_{12} = \sigma_{23} = 0 \text{ at } x_i \in S_2; \ \sigma_{ij} n_j = 0 \text{ at } x_i \in S_3,$$

where x_i is the spatial coordinates, S_1 is the outer surface of the fixed wall, l is the size of the unit cell, S_2 is the outer surface of the loaded wall, S_3 is the surfaces of the side walls of the cell and all other surfaces of rings and ligaments that do not belong to S_1 and S_2, and n_j is the component of the normal vector to surface S_3.

It is assumed that the initial stresses and strains are equal to zero:

$$\sigma_{ij}(t_0) = \varepsilon_{ij}(t_0) = 0.$$

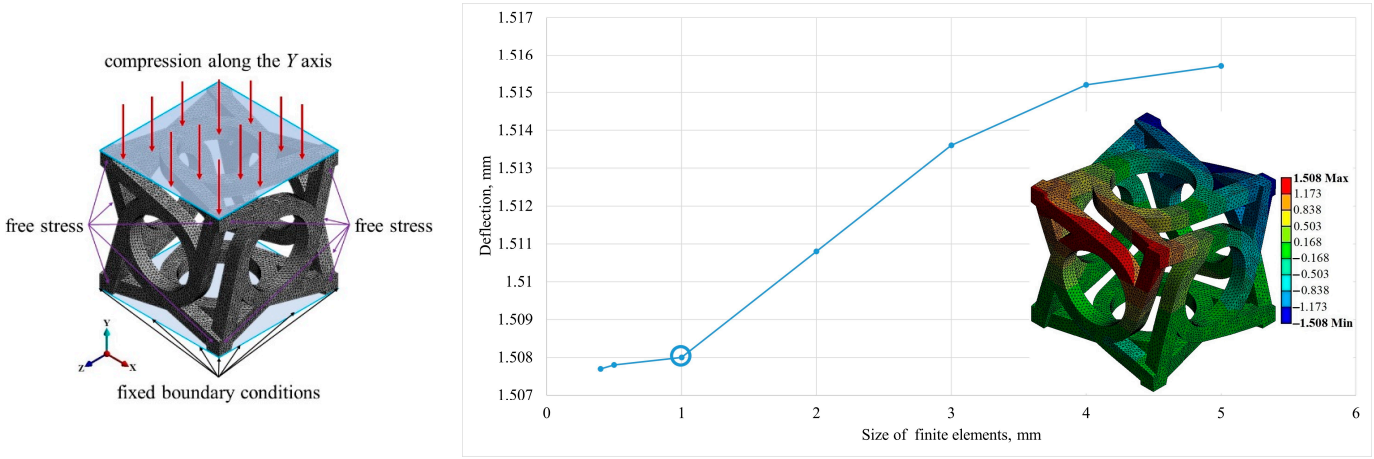

(**a**) (**b**)

Figure 3. (**a**) Finite element model of the studied unit cell with the loading conditions applied and (**b**) mesh convergence in terms of the deflection of the upper wall vertices with the image of a unit cell with the deflection distribution according to the color scale.

2.4. Computational Model

Numerical simulations are performed by finite element modeling using the commercial ANSYS Ansys WB 2020R2 software. A unit cell is considered the system of rods or beams, which is modeled as a set of three-dimensional solid elements in finite element calculations. The sample is deformed without contact interaction of its constituent elements. Simulation is implemented within large deflection theory.

When developing a numerical model, it is important to perform the mesh convergence analysis to obtain reliable results, as well as to reduce computational costs. The mesh convergence study suggests that physics-based finite element size gives the best estimates of mechanical properties within the context of this work. Since our main interest is in the description of the torsion of a metamaterial sample, the mesh convergence is analyzed in terms of the deflection of the upper wall of the sample. During the analysis, the element size decreased from 5 to 0.4 mm. Three-dimensional finite element models consist of tetrahedral elements, as shown in Figure 3. According to the mesh convergence analysis performed, the average mesh element size is 1 mm.

To make sure that the size of the generated mesh is chosen correctly, extrapolation methods can be used for error calculation [26]. The results of the extrapolation analysis show that the computational error at the chosen mesh spacing is 0.37%.

3. Results

The problem to be solved in the present paper is the influence of topological defects in the unit cell of a metamaterial on its properties. The quantities to be determined are the nontrivial response, i.e., torsion of samples, and the effective Young's modulus.

3.1. Mechanism of Structure Rotation and Sample Torsion

A distinctive property of the tetrachiral metamaterial is the tension/compression–torsion coupling effect during its deformation. Uniaxial loading of a unit cell is accompanied by its torsion about the loading axis (compression–torsion coupling effect). This process is caused by the rotation of tetrachiral structures. The rotation of each tetrachiral structure is determined by the direction of chirality. Since the unit cell has six walls, the rotation of each wall ω_i contributes to the total torsion $\boldsymbol{\alpha}$:

$$\boldsymbol{\alpha} = \alpha(\omega_i),\ i = 1, 2, \ldots, 6.$$

The conventional analysis of deformation mechanisms is based on kinematic structural analysis [27]. To do this, it is necessary to know the displacements of each part of the structure under deformation. In the investigation of the compression–torsion coupling effect, the vector of the sample torsion is expressed based on the displacement formula [28]. The torsion angle in degrees can also be determined from deflection by the formula [29,30].

$$\alpha_y = \left(\frac{180}{\pi}\right)\arcsin\left(\frac{2\Delta x}{l}\right) = \left(\frac{180}{\pi}\right)\arcsin\left(\frac{2\Delta z}{l}\right),$$

where Δx and Δz are the displacements of the wall vertices along the X- and Z-axes, respectively, and l is the length of the unit cell.

A unit cell with a regular arrangement of tetrachiral structures (Figure 4) is assumed to be defect-free (a cell without topological defects) and is denoted by ω_0. When looking from within the cell (Figure 4a), the direction of chirality is the same on each wall (counterclockwise).

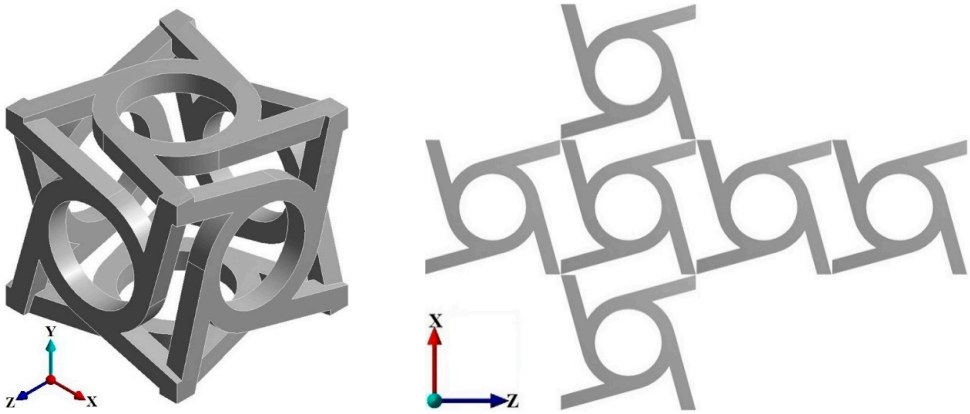

(**a**) (**b**)

Figure 4. Cubic unit cell with a regular arrangement of tetrachiral structures: (**a**) in space and (**b**) in a plane.

Under uniaxial loading along one of the three orthogonal axes, the vertices of the moving wall of a cubic cell are displaced along the other two axes. For example, under loading along the Y-axis, the vertex deflections along the X- and Z-axes due to the cell torsion are equal and take on the values of +1.51 mm (in the positive direction) and −1.51 mm (in the negative direction). Similar values of vertex displacements are observed under loading along the other two axes.

Next, we study the compression–torsion coupling effect in chiral structures with topological defects. Topological defects reveal themselves in the change of the direction of chirality in the walls of the cubic cell (Figure 5). Changes occur in the following sequence:

regular (initial) unit cell, ω_0 (Figure 4);
the direction of chirality changes in the upper wall, ω_1 (Figure 5a);
in unit cell ω_1, the direction of chirality changes in the lower wall, ω_2 (Figure 5b);
in unit cell ω_2, the direction of chirality changes in the left wall, ω_3 (Figure 5c);
in unit cell ω_3, the direction of chirality changes in the right wall, ω_4 (Figure 5d);
in unit cell ω_4, the direction of chirality changes in the front wall, ω_5 (Figure 5e);
in unit cell ω_5, the direction of chirality changes in the back wall, ω_6 (Figure 5f).

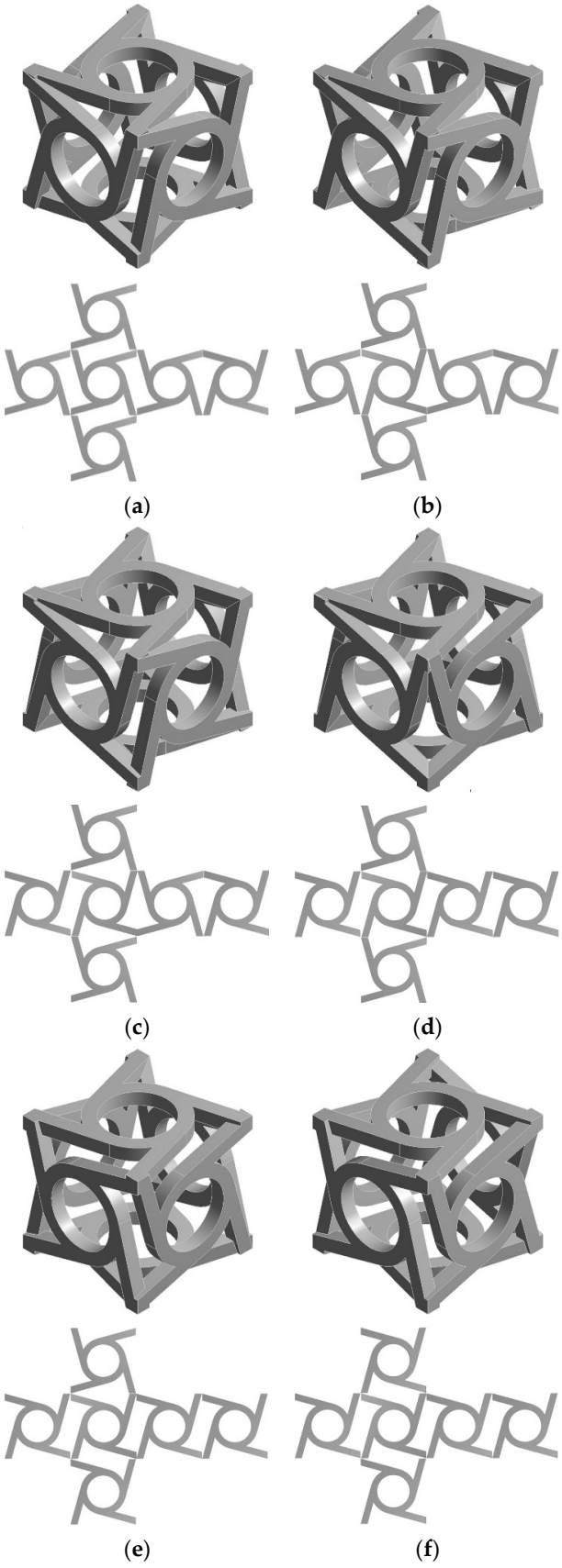

Figure 5. Sequence of changes in the direction of chirality of a unit cell: changes occur in one (**a**), two (**b**), three (**c**), four (**d**), five (**e**), and six (**f**) walls.

Under the uniaxial loading of a metamaterial unit cell, tetrachiral structures in the walls rotate and contribute to the total torsion of the cell. The initial (defect-free) unit cell can be described as an orthotropic body. The introduction of topological defects associated with changes in the wall chirality affects the cell torsion value. Moreover, torsion values depend on the loading direction. Therefore, the response of unit cells with the same topological defects to compression is studied under loading along three orthogonal axes (Figure 6). Figure 6 shows how this influences the compression–torsion coupling effect. Both an increase and a decrease are observed in this effect. In structures with certain topological defects, displacements are asymmetric. One such example is the case of loading along the *Z*-axis and deflection along the *Y*-axis, which is plotted on the far right of Figure 6. Under loading of unit cell ω_3, the positive deflection along the *Y*-axis increases by 65%. The negative deflection also changes; it decreases by 24%, which is disproportional and indicates that the cell experiences not so much torsion as shear. In the transition from ω_3 to ω_4, the absolute values of both the maximum and minimum deflections increase by 36% as compared to initial cell ω_0. Thus, the range is kept symmetrical.

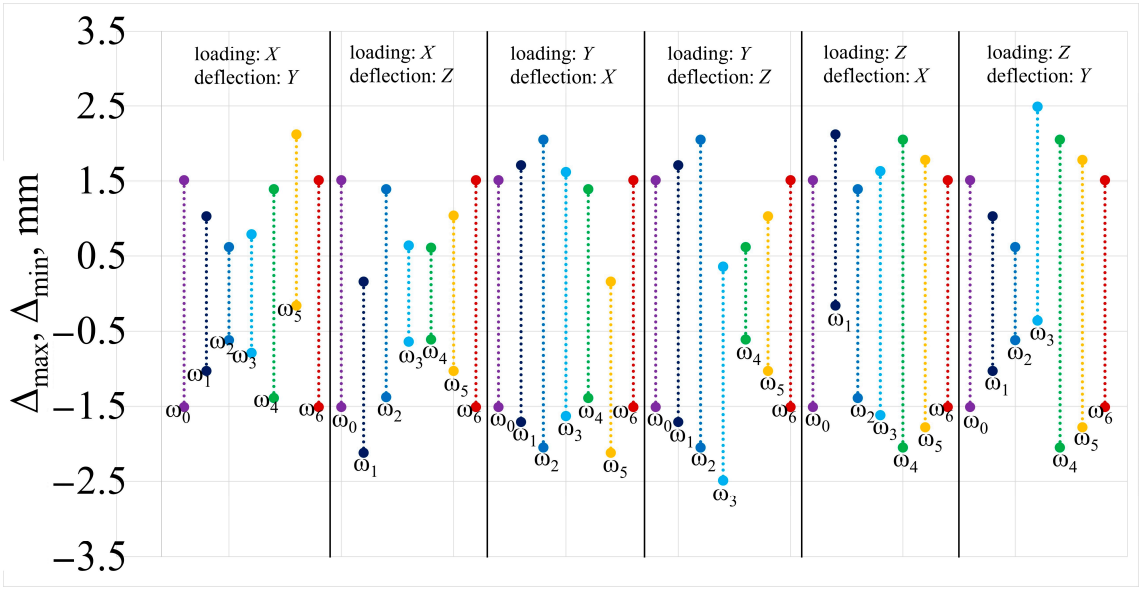

Figure 6. Deflection of the surface with the nonzero kinematic boundary condition under loading in the three orthogonal directions (*X*, *Y*, *Z*).

Then, we focus on the case of loading along the *Y*-axis (Figure 7) to clarify how the topological defects affect the compression–torsion coupling effect of the unit cell. The change in the direction of rotation of the upper wall of unit cell ω_1 leads to a symmetrical increase of the absolute values of deflection in the *XZ* plane. It is seen that unit cells with defects in the upper and side walls rotate in the same direction, which enhances the compression–torsion coupling effect (Δ = 1.71 mm). The change in the direction of rotation of the lower wall further increases torsion (2.05 mm). The change in the rotation of the left wall reduces the deflection to 1.62 mm as it hinders the cell torsion. The rotation of the right wall reduces the compression–torsion coupling effect from the previous case (1.39 mm). The change in the front wall results in almost zero deflection (0.16 mm). This is due to the symmetrical rotation of the front and back walls, which causes the sample shear. The upper wall is shifted relative to the lower one in the negative direction along the *X*-axis. At last, the change in the back wall leads to the regular arrangement of the wall structures. In this case, the value of torsion is equal to the initial one, but its direction reverses.

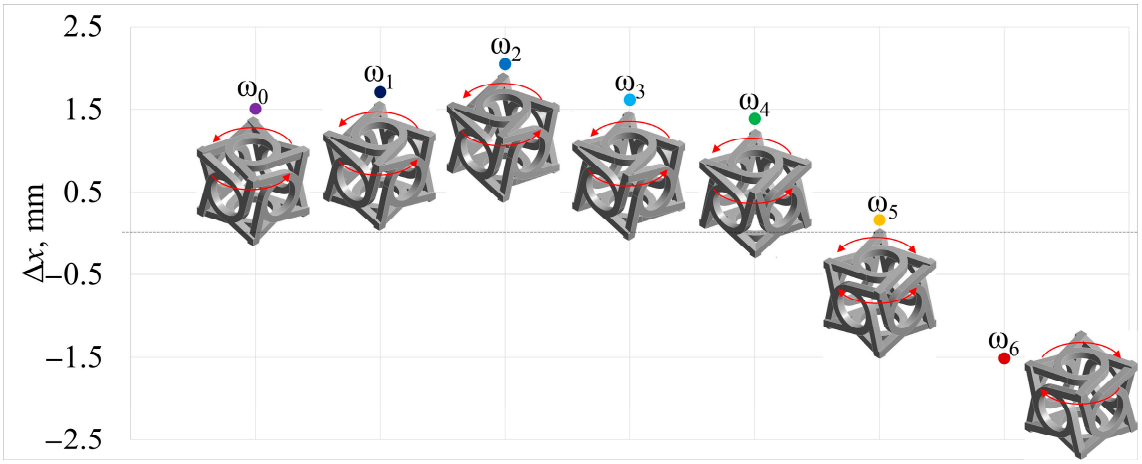

Figure 7. Deflection of the upper wall in unit cells with spatially different structures (the arrows show the direction of torsion or shear of the sample).

The introduction of defects causes a wide variety of changes in mechanical behavior. As shown in [14,15,31–33], this affects the physical and mechanical properties. Therefore, the dependence of Young's modulus on the topological defects in the unit cell of the metamaterial will be considered below.

3.2. Relative Effective Young's Modulus of the Metamaterial, E/E_{bm}

The phenomenon of torsion of tetrachiral metamaterials under uniaxial loading makes it possible to change the effective Young's modulus by choosing the optimum cell-to-ring ratio. Figure 8 shows the value range of the effective Young's modulus E relative to Young's modulus of the base material, E_{bm}. The effective Young's modulus is determined by the following formula:

$$E = \frac{\frac{F}{S}}{\frac{\Delta l}{l}},$$

where F is the support reaction force of the fixed wall, S is the cross-section of the cubic unit cell, Δl is the displacement after longitudinal compression by 3%, and l is the unit cell length.

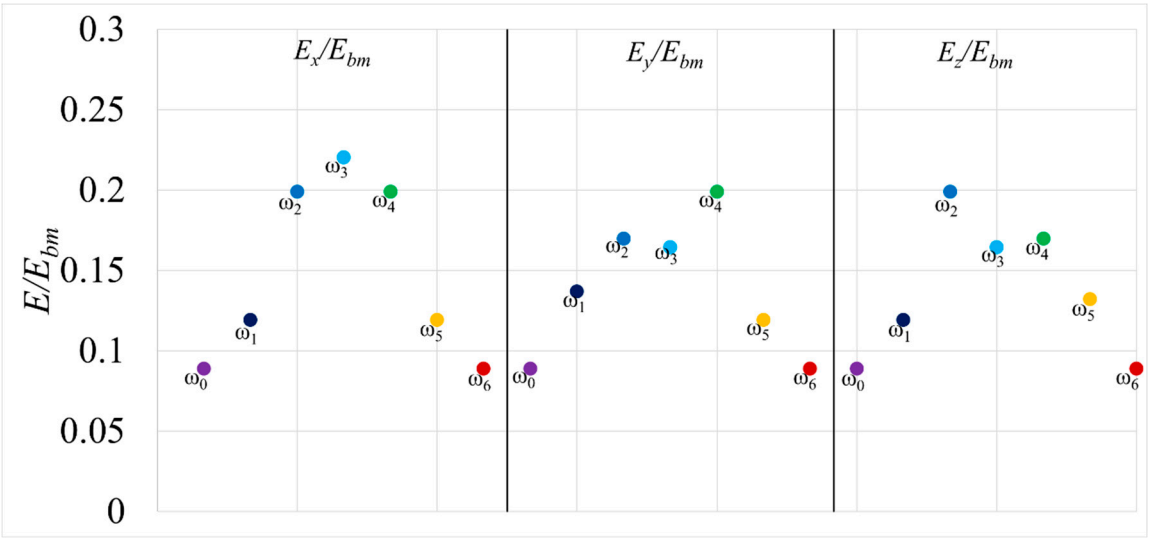

Figure 8. Relative effective Young's modulus of the metamaterial under loading along three orthogonal axes with the introduction of topological defects in its unit cell.

Let us consider the case of loading along the *X*-axis. Three levels are distinguished in the *E* values. The introduction of one topological defect leads to an increase in Young's modulus by 34%. Further changes (unit cells ω_2 and ω_3) result in an increase in *E* by 124% and 148% as compared to the regular structure, respectively. In this case, the specific volume of the base material changes insignificantly, tending to a value of 0.2:

$$\rho_{rel} = \frac{\rho_{mm}}{\rho_{bm}} = \frac{\frac{m_{bm}}{V_s}}{\rho_{bm}} = \frac{\frac{V_{bm} \cdot \rho_{bm}}{l \cdot l \cdot l}}{\rho_{bm}} = \frac{V_{bm}}{l \cdot l \cdot l} = \frac{25147 \text{ mm}^3}{50 \text{ mm} \cdot 50 \text{ mm} \cdot 50 \text{ mm}} = 0.2,$$

where ρ_{mm} is the average density of the metamaterial, ρ_{bm} is the density of the base material, m_{bm} is the mass of the base material, V_s is the sample volume (volume of the base material and pore space), V_{bm} is the volume of the base material, and l is the unit cell length.

The data derived for the relative Young's modulus of the metamaterial under loading along the *Y*- and *Z*-axes turn out to be symmetrical with respect to the vertical line that separates them. Similar dependencies were also observed in Figure 6, particularly in the following cases: (1) loading along axis *Y* and deflection along axis *Z*; (2) loading along axis *Z* and deflection along axis *Y*. Most likely, this is due to the "symmetrical" relationship between the loading axis and the set of walls with defects.

3.3. Further Actions

In this paper, an attempt is made to describe the influence of topological defects in the unit cell of a metamaterial on its properties. The analysis results can be used to develop algorithms for considering such rearrangements in the metamaterial structure. Then, one can proceed to defects of a larger length scale in metamaterial samples. It is expected that this will help develop the laws of topological optimization of the cellular structures of metamaterials. In future works, we are planning to study other topological defects, in particular in metamaterial samples.

4. Discussion

As was demonstrated in [25], a defect-free unit cell of tetrachiral metamaterial possessed the orthotropy of mechanical properties. The results presented here show that this is not the case for unit cells with topological defects in their walls.

The derived numerical results can be used to determine the correlation of the two quantities under study (deflection and effective Young's modulus). Table 2 shows how the studied characteristics change during topological rearrangements, revealing their correlation. It is seen that, as the number of topological defects in a unit cell grows to two, the deflection from the initial position increases. At the same time, there should be an increase in the force to ensure the corresponding strain. With a change in the chirality of the third wall (ω_3), the deflection value decreases, but the expected decrease in *E* does not occur. A further increase in the number of defects affects the studied characteristics in different ways. The introduction of two more defects in the walls leads to a decrease in torsion and an increase in Young's modulus, after which both characteristics decrease. This phenomenon is caused by the fact that adjacent chiral structures rotate in different directions, which complicates the cell deformation, thus preventing the compression–torsion coupling effect. It is expected that, when the chirality of all walls changes, the effective Young's modulus is equal to that of the initial structure, and the deflection is equal in absolute value but has the opposite sign.

Table 2. Tetrachiral structure parameters.

Topological Defect	ω_0	ω_1	ω_2	ω_3	ω_4	ω_5	ω_6
Deflection, mm	1.51	1.71	2.05	1.62	1.39	0.16	–1.51
Young's modulus, MPa	23	36	44	43	52	31	23

Ji et al. [34] and Pabst and Gregorová [35], in a preview of scaling laws, suggested that the relative effective mechanical properties of the porous lattice structures are functions of their bulk porosity and microstructural characteristics [3,8], and this suggestion is supported by other related works [23,36], etc. That is why the results in Table 2 are given for cells of the same specific volume (porosity).

5. Conclusions

This paper dealt with the behavior of a mechanical tetrachiral metamaterial. The key point was the introduction of topological defects into the unit cell (changing the direction of chirality). To study the influence of the introduced topological defects, consideration was given to the mechanical behavior of unit cells, in particular, the rotation of their walls. The influence of these structural defects on the effective elastic mechanical properties of tetrachiral cellular structures was also found. The correlation between the elastic effective mechanical properties and the topological arrangement of tetrachiral structures was determined.

Under loading along three orthogonal axes, a defect-free unit cell did not change its physical and mechanical properties, which indicates the orthotropy of properties. The same properties were found in the cell with defects in all six walls. However, the torsion in this cell was opposite in sign to that in the cell without defects. Consequently, this unit cell can also be treated as orthotropic. Intermediate structures led to corresponding changes in physical and mechanical properties. A change in the direction of chirality in the cell walls perpendicular to the loading axis can either increase or decrease the compression–torsion coupling effect.

The influence of different topological defects as well as of loading along three orthogonal axes on the effective Young's modulus was studied. The highest value of E was found to be 57 MPa.

The present paper points to the necessity of consideration for the metamaterial structure as well as for its topological arrangement, in particular topological defects. The results obtained confirmed the close relationship between microstructural geometry and mechanical deformation. The introduction of topological defects into metamaterial structures plays a key role in controlling their behavior. It was shown that a topological defect in a unit cell of a tetrachiral metamaterial strongly determines its torsional behavior.

Author Contributions: Conceptualization, L.A.; methodology, L.A. and I.S.; formal analysis, E.K.; investigation, L.A., K.I. and E.K.; writing—original draft preparation, L.A.; writing—review and editing, L.A. and I.S.; project administration, L.A.; funding acquisition, L.A. All authors have read and agreed to the published version of the manuscript.

Funding: "This research was funded by the Development Program of Tomsk State University (Priority-2030)" and "The APC was funded by the Development Program of Tomsk State University (Priority-2030)".

Data Availability Statement: Data are contained within the article.

Conflicts of Interest: The authors declare no conflict of interest. The funders had no role in the design of the study; in the collection, analyses, or interpretation of data; in the writing of the manuscript; or in the decision to publish the results.

References

1. Tan, T.; Yan, Z.; Zou, H.; Ma, K.; Liu, F.; Zhao, L.; Peng, Z.; Zhang, W. Renewable Energy Harvesting and Absorbing via Multi-Scale Metamaterial Systems for Internet of Things. *Appl. Energy* **2019**, *254*, 113717. [CrossRef]
2. Cummer, S.A.; Christensen, J.; Alù, A. Controlling Sound with Acoustic Metamaterials. *Nat. Rev. Mater.* **2016**, *1*, 16001. [CrossRef]
3. Sangsefidi, A.R.; Kadkhodapour, J.; Anaraki, A.P.; Dibajian, S.H.; Schmauder, S. Enhanced Energy Harvesting by Devices with the Metamaterial Substrate. *Phys. Mesomech.* **2022**, *25*, 568–582. [CrossRef]
4. Yu, X.; Zhou, J.; Liang, H.; Jiang, Z.; Wu, L. Mechanical Metamaterials Associated with Stiffness, Rigidity and Compressibility: A Brief Review. *Prog. Mater. Sci.* **2018**, *94*, 114–173. [CrossRef]
5. Akhmetshin, L.R.; Smolin, I.Y. Analysis of Some Methods of Integration of Cells in a Mechanical Metamaterial. *Tomsk. State Univ. J. Math. Mech.* **2022**, *77*, 27–37. [CrossRef]
6. Zhang, X.; Wu, Y. Effective Medium Theory for Anisotropic Metamaterials. *Sci. Rep.* **2015**, *5*, 7892. [CrossRef]

7. Jenett, B.E. Discrete Mechanical Metamaterials. Ph.D. Thesis, Massachusetts Institute of Technology, Cambridge, MA, USA, September 2020. Available online: https://hdl.handle.net/1721.1/130610 (accessed on 2 October 2023).
8. Fu, M.-H.; Zheng, B.-B.; Li, W.-H. A Novel Chiral Three-Dimensional Material with Negative Poisson's Ratio and the Equivalent Elastic Parameters. *Compos. Struct.* **2017**, *176*, 442–448. [CrossRef]
9. Frenzel, T.; Kadic, M.; Wegener, M. Three-Dimensional Mechanical Metamaterials with a Twist. *Science* **2017**, *358*, 1072–1074. [CrossRef]
10. Grima, J.N.; Gatt, R.; Farrugia, P.-S. On the Properties of Auxetic Meta-Tetrachiral Structures. *Phys. Stat. Sol. (B)* **2008**, *245*, 511–520. [CrossRef]
11. Prall, D.; Lakes, R.S. Properties of a Chiral Honeycomb with a Poisson's Ratio of—1. *Int. J. Mech. Sci.* **1997**, *39*, 305–314. [CrossRef]
12. Wu, Q.; Xu, X.; Qian, H.; Wang, S.; Zhu, R.; Yan, Z.; Ma, H.; Chen, Y.; Huang, G. Active metamaterials for realizing odd mass density. *Proc. Natl. Acad. Sci. USA* **2023**, *120*, e2209829120. [CrossRef] [PubMed]
13. Xia, W.; Oterkus, E.; Oterkus, S. 3-Dimensional Bond-Based Peridynamic Representative Volume Element Homogenization. *Phys. Mesomech.* **2021**, *24*, 541–547. [CrossRef]
14. Zuev, L.B.; Khon, Y.A. Plastic Flow as Spatiotemporal Structure Formation. Part I. Qualitative and Quantitative Patterns. *Phys. Mesomech.* **2022**, *25*, 103–110. [CrossRef]
15. Meeussen, A.S.; Oğuz, E.C.; Shokef, Y.; Hecke, M.V. Topological Defects Produce Exotic Mechanics in Complex Metamaterials. *Nat. Phys.* **2020**, *16*, 307–311. [CrossRef]
16. Meeussen, A.S.; Oğuz, E.C.; Hecke, M.V.; Shokef, Y. Response Evolution of Mechanical Metamaterials under Architectural Transformations. *New J. Phys.* **2020**, *22*, 023030. [CrossRef]
17. Bonfanti, S.; Guerra, R.; Zaiser, M.; Zapperi, S. Digital Strategies for Structured and Architected Materials Design. *APL Mater.* **2021**, *9*, 020904. [CrossRef]
18. Maconachie, T.; Leary, M.; Lozanovski, B.; Zhang, X.; Qian, M.; Faruque, O.; Brandt, M. SLM lattice structures: Properties, performance, applications and challenges. *Mater. Des.* **2019**, *183*, 108137. [CrossRef]
19. Bhullar, S.K.; Lala, N.L.; Ramkrishna, S. Smart Biomaterials—A Review. *Rev. Adv. Mater. Sci.* **2015**, *40*, 303–314.
20. Giannini, D.; Schevenels, M.; Reynders, E.P.B. Rotational and Multimodal Local Resonators for Broadband Sound Insulation of Orthotropic Metamaterial Plates. *J. Sound Vib.* **2023**, *547*, 117453. [CrossRef]
21. Giorgio, I.; Hild, F.; Gerami, E.; dell'Isola, F.; Misra, A. Experimental Verification of 2D Cosserat Chirality with Stretch-Micro-Rotation Coupling in Orthotropic Metamaterials with Granular Motif. *Mech. Res. Commun.* **2022**, *126*, 104020. [CrossRef]
22. Feng, N.; Tie, Y.; Wang, S.; Guo, J. A Novel 3D Bidirectional Auxetic Metamaterial with Lantern-Shape: Elasticity Aspects and Potential for Load-Bearing Structure. *Compos. Struct.* **2023**, *321*, 117221. [CrossRef]
23. Pan, C.; Han, Y.; Lu, J. Design and Optimization of Lattice Structures: A Review. *Appl. Sci.* **2020**, *10*, 6374. [CrossRef]
24. Akhmetshin, L.; Smolin, I. Characterization of a Chiral Metamaterial Depending on the Type of Connection between Unit Cells. *Proc. Inst. Mech. Eng. C J. Mech. Eng. Sci.* **2022**, *236*, 10214–10220. [CrossRef]
25. Akhmetshin, L.; Iokhim, K.; Kazantseva, E.; Smolin, I. Response Evolution of a Tetrachiral Metamaterial Unit Cell under Architectural Transformations. *Symmetry* **2022**, *15*, 14. [CrossRef]
26. Sofroniou, M.; Spaletta, G. Extrapolation Methods in Mathematica. *J. Numer. Anal. Ind. Appl. Math.* **2008**, *3*, 105–121.
27. Li, X.; Yang, Z.; Lu, Z. Design 3D Metamaterials with Compression-Induced-Twisting Characteristics Using Shear–Compression Coupling Effects. *Extreme Mech. Lett.* **2019**, *29*, 100471. [CrossRef]
28. Xu, W.; Liu, Z.; Wang, L.; Zhu, P. 3D Chiral Metamaterial Modular Design with Highly-Tunable Tension-Twisting Properties. *Mater. Today Commun.* **2022**, *30*, 103006. [CrossRef]
29. Wang, H.; Zhang, C.; Qin, Q.-H.; Bai, Y. Tunable Compression-Torsion Coupling Effect in Novel Cylindrical Tubular Metamaterial Architected with Boomerang-Shaped Tetrachiral Elements. *Mater. Today Commun.* **2022**, *31*, 103483. [CrossRef]
30. Akhmetshin, L.R.; Smolin, I.Y. Effect of the Type of Unit Cell Connection in a Metamaterial on Its Programmable Behavior. *Nanosci. Technol. Int. J.* **2023**, *14*, 63–71. [CrossRef]
31. Jin, L.; Khajehtourian, R.; Mueller, J.; Rafsanjani, A.; Tournat, V.; Bertoldi, K.; Kochmann, D.M. Guided Transition Waves in Multistable Mechanical Metamaterials. *Proc. Natl. Acad. Sci. USA* **2020**, *117*, 2319–2325. [CrossRef]
32. Coulais, C.; Teomy, E.; De Reus, K.; Shokef, Y.; Van Hecke, M. Combinatorial Design of Textured Mechanical Metamaterials. *Nature* **2016**, *535*, 529–532. [CrossRef] [PubMed]
33. Wang, Z.-P.; Wang, Y.; Poh, L.H.; Liu, Z. Integrated Shape and Size Optimization of Curved Tetra-Chiral and Anti-Tetra-Chiral Auxetics Using Isogeometric Analysis. *Compos. Struct.* **2022**, *300*, 116094. [CrossRef]
34. Ji, S.; Gu, Q.; Xia, B. Porosity Dependence of Mechanical Properties of Solid Materials. *J. Mater. Sci.* **2006**, *41*, 1757–1768. [CrossRef]
35. Pabst, W.; Gregorová, E. Critical Assessment 18: Elastic and Thermal Properties of Porous Materials—Rigorous Bounds and Cross-Property Relations. *Mater. Sci. Technol.* **2015**, *31*, 1801–1808. [CrossRef]
36. Choren, J.A.; Heinrich, S.M.; Silver-Thorn, M.B. Young's Modulus and Volume Porosity Relationships for Additive Manufacturing Applications. *J. Mater. Sci.* **2013**, *48*, 5103–5112. [CrossRef]